Aquatic Geochemistry **6:** 65–86, 2000.

Remineralization Ratios in the Subtropical North Pacific Gyre

YUAN-HUI LI, DAVID M. KARL, CHRISTOPHER D. WINN, FRED T. MACKENZIE and KATHLEEN GANS
Department of Oceanography, University of Hawaii, Honolulu, Hawaii, 96822

(Received: 20 July 1998; accepted: 3 September 1999)

Abstract. Based on a new mixing model of two end-members, the water column remineralization ratios of $P/N/C_{org} - O_2 = 1/13 \pm 1/135 \pm 18/170 \pm 9$ are obtained for the Hawaii Ocean Time-series (HOT) data set at station ALOHA. The traditional Redfield ratios of $P/N/C_{org}/-O_2 = 1/16/106/138$ have standard deviations of more than 50%, when they are based on the average composition of phytoplankton. Apparently, the remineralization processes in the water column have smoothed out the observed large variability of plankton compositions. A new molar formula for the remineralized plankton may be written as $C_{135}H_{280}O_{105}N_{13}P$ or $C_{25}(CH_2O)_{101}(CH_4)_9(NH_3)_{13}(H_3PO_4)$. Oxidation of this formula results in

$$C_{25}(CH_2O)_{101}(CH_4)_9(NH_3)_{13}(H_3PO_4) + 170O_2 \rightarrow 135CO_2 + 132H_2O + 13NO_3^- + H_2PO_4^- + 14H^+.$$

For comparison, remineralization using Redfield's formula gives:

$$(CH_2O)_{106}(NH_3)_{16}(H_3PO_4) + 138O_2 \rightarrow 106CO_2 + 122H_2O + 16NO_3^- + H_2PO_4^- + 17H^+$$

Key words: Mixing model, preformed nutrients, Redfield ratios, Remineralization ratios

1. Introduction

Based on the chemical composition data of plankton in the ocean (Fleming, 1940), Redfield et al. (1963) proposed an idealized molar formula of $(CH_2O)_{106}(NH_3)_{16}(H_3PO_4)$ to represent average plankton. Decomposition of one mole of idealized plankton can be represented by the overall net reaction of:

$$(CH_2O)_{106}(NH_3)_{16}(H_3PO_4) + 138O_2 \rightarrow 106CO_2 + 122H_2O + 16NO_3^-$$

$$+ H_2PO_4^- + 17H^+$$

The intermediate steps may include the remineralization of particulate organic matter (such as dead plankton, marine snow, fecal pellets, etc.) and the much larger pool of dissolved and colloidal organic matter. The remineralization processes

occur mainly in the water column, but the fluxes of remineralized products from the sediment interstitial water to the overlying water can be important, especially in coastal regions. For simplicity, biogeochemistry of these intermediate steps is omitted here. The molar ratios among the remineralized P, N, C_{org}, and the consumed O_2, are P/ N/C_{org}/–O_2 = 1/ 16/ 106 /138 and are known as the "traditional Redfield ratios". Unfortunately, the uncertainties of these average ratios based either on the average composition of plankton or on the water column chemistry are not given. The negative sign before O_2 implies consumption of oxygen during oxidation of organic compounds. Also, we may define the following ratios of the changes in reactant and product constituents:

$$r_p = -\mathrm{O_2/P} = 138,$$

$$r_n = -\mathrm{O_2/N} = 138/16 = 8.6,$$

$$r_c = -\mathrm{O_2/C_{org}} = 138/106 = 1.30,$$

and

$$a = \mathrm{H^+/C_{org}} = (1/r_p + 1/r_n)r_c = 17/106 = 0.16.$$

where r_p, r_n, and r_c are respectively the molar ratios of the consumed O_2 to the remineralized P, N, and C_{org}; and "a" is the molar ratio of the produced H^+ to the remineralized C_{org}. The given values for the above parameters apply only to the decomposition of idealized plankton. Also the value of 0.16 for "a" represents a reduction of 0.16 equivalent of alkalinity in seawater due to decomposition of one mole of idealized planktonic carbon (Brewer et al., 1975). The hydrogen ion is mainly produced by oxidation of organic NH_3 and some slight dissociation of phosphoric acid. One can easily show the following relationship, when all ratios are normalized to the remineralized phosphate:

$$\mathrm{P{:}\ N{:}\ C_{org} : -O_2} = 1 : (r_p/r_n) : (r_p/r_c) : r_p$$

The Redfield ratios in the ocean were re-evaluated recently, mainly based on the GEOSECS (Geochemical Ocean Section Study) data and mixing models that employ one and two end-members along an isopycnal horizon or a neutral surface. The results suggested a need to modify the traditional Redfield ratios of remineralization, especially for the –O_2/P ratio (= r_p). For example, Takahashi et al. (1985) suggested an –O_2/P ratio of 172 along isopycnals in the thermocline. Broecker et al. (1985) and Peng and Broecker (1987) obtained an –O_2/P ratio of 175 ± 5, independent of water depth. In contrast, Minster and Boulahdid (1987) and Boulahdid and Minster (1989) suggested a decrease in the –O_2/P ratio from about 172 in the thermocline down to about 115 at the bottom. Anderson and Sarmiento (1994) applied a nonlinear inverse method to nutrient data along a neutral surface to estimate

simultaneously the remineralization ratios. Their ratios of P/ $N/C_{org}/-O_2$ are 1/16 $\pm$ 1/117 $\pm$ 14/170 $\pm$ 10 at depths between 400 m and 4000 m. They also suggested a reduction of N/P ratio to 12 $\pm$ 2 between 1000 m and 3000 m due to sedimentary denitrification. The high $-O_2/P$ ratio of 170 $\pm$ 10 indicates oxidation of organic compounds that were, on average, more reduced than carbohydrates (Peng and Broecker, 1987). Anderson's (1995) new estimate of the average stoichiometry of marine phytoplankton ($C_{106}H_{175\pm11}O_{42\pm6}N_{16}P$) gives the $-O_2/P$ ratio of 150 $\pm$ 10 according to the following reaction:

$$C_{106}H_{175}O_{42}N_{16}P + 150O_2 \rightarrow 106CO_2 + 78H_2O + 16NO_3^- + H_2PO_4^- + 17H^+.$$

In this paper, we develop a simple mixing model of two end-members to estimate the remineralization ratios of $P/N/C_{org}/-O_2$ in the water column at station ALOHA. It is common knowledge that horizontal advection and diffusion are much faster than vertical processes. However, when normalized to the scale of distance, the horizontal and vertical processes become equally important (Fiadeiro and Craig, 1978). For example, the mean vertical distance of the deep ocean is about 3 km (z), and the horizontal distance scale in the Pacific Ocean is in the order of about 10000 km (x), so x/z is about 3300. Fiadeiro and Craig (1978) gave horizontal and vertical eddy diffusion constants of $K_h = 5 \cdot 10^6$ cm^2/sec and K_v = 0.6 cm^2/sec for the deep ocean, therefore, $(K_h/K_v)^{1/2}$ = 3000 (because average diffusive distance = $(2K \cdot t)^{1/2}$), which is close to the x/z value here. In short, both horizontal and vertical diffusive mixing affect about the same fraction of the respective distance in a given time interval. Fiadeiro and Craig (1978) also gave a uniform vertical upwelling velocity of 3 m/yr to balance out the horizontal advection of about 10 Sv (10^7 m^3/s) seawater into the Pacific Ocean basin. Both give the water mean residence time of about 1000 years in the deep Pacific Ocean. In short, one can extract the remineralization ratios from a vertical profile data set and from an interpolated data set along an isopycnal horizon or neutral surface, as long as the chosen data set form a straight line in a θ-S diagram as will be shown later. The vertical profiles of nutrient data used in the present work are obtained from the Hawaii Ocean Time-series (HOT) program at station ALOHA (Karl and Lukas, 1996). The remineralization ratios obtained from the present work are compared to the results of recent studies, and their biogeochemical implications for the nitrogen fixation/denitrification processes and the dissolution of carbonates/oxidation of organic matter in the water column are discussed.

2. Two End-member Mixing Model

In a plot of the conservative tracers salinity (S) versus potential temperature (θ) for a vertical profile, a linear segment can be interpreted as representing two end-member mixing of water types. The potential temperature (θ) of any water sample on this linear segment can be expressed by:

$$\theta = f \cdot \theta_1 + (1 - f) \cdot \theta_2; \qquad \text{i.e., } f = (\theta - \theta_2)/(\theta_1 - \theta_2), \tag{1}$$

where θ_1 and θ_2 are the potential temperatures of the end members 1 and 2, and f is the fraction of end member 1 in the water sample; thus, $(1 - f)$ is the fraction of end-member 2. In principle, one can also obtain f from the salinity data.

Similarly, a conservative tracer "NO" (=O_2 + $r_n \cdot NO_3$; Broecker, 1974) of the water sample on the linear segment of the mixing line is:

$$(NO) = O_2 + r_n \cdot NO_3 = f \cdot (NO)_1 + (1 - f) \cdot (NO)_2, \tag{2a}$$

and by rearrangement:

$$O_2 = (NO)_2 + [(NO)_1 - (NO)_2] \cdot f - r_n \cdot NO_3, \tag{2b}$$

where $(NO)_1$ and $(NO)_2$ are the "NO" values for the end-members 1 and 2.

By substituting Equation (1) into Equation (2b), one obtains:

$$O_2 = \alpha_0 + \alpha_1 \cdot \theta - r_n \cdot NO_3, \tag{2c}$$

where

$$\alpha_0 = (NO)_2 - [(NO)_1 - (NO)_2] \cdot \theta_2/[\theta_1 - \theta_2],$$

and

$$\alpha_1 = [(NO)_1 - (NO)_2]/[\theta_1 - \theta_2].$$

By the multiple linear regression of O_2, θ, and NO_3 concentration data from the linear segment, one can estimate α_0, α_1 and r_n without explicitly knowing the individual end-member values for θ and "NO". This approach applies equally well to another conservative tracer "PO" (=O_2 + $r_p \cdot PO_4$; Broecker, 1974, Broecker et al., 1985) to obtain r_p. For this method to work properly, O_2 concentration data from the selected segment should exhibit a curvature in a plot of O_2 versus θ. As is clear from Equation (2c), if the plot of O_2 versus θ is near linear, r_n becomes very small and has a large uncertainty. For the multiple linear regression, one may use the SPSS (Statistical Package for the Social Sciences) and the SAS (Statistical Analysis System) PC programs or other software. Once r_n and r_p are known, one can calculate "NO", "PO", and the preformed nitrate (NO_3^0) and phosphate (PO_4^0) of any water sample on the linear segment of the mixing curve according to:

$$NO_3^0 = NO_3 - AOU/r_n, \tag{3a}$$

and

$$PO_4^0 = PO_4 - AOU/r_p, \tag{3b}$$

where AOU is the apparent oxygen utilization (=$O_2^0 - O_2$), and O_2^0 is the saturated oxygen concentration at the given S and θ of the water sample in equilibrium with

air. Whenever AOU is zero in the surface ocean, the concentrations of nitrate and phosphate represent the preformed values.

For the total dissolved inorganic carbon (DIC, in units of μmol/kg) and titration alkalinity (Alk, in units of μeq/kg) data, the following relationships hold:

$$\mathrm{DIC} - \mathrm{DIC}^0 = x + y, \tag{4a}$$

$$\mathrm{Alk} - \mathrm{Alk}^0 = 2x - a \cdot y, \tag{4b}$$

and

$$\mathrm{AOU} = r_c \cdot y, \tag{4c}$$

where DIC^0 and Alk^0 are the preformed DIC and Alk in the water column; and x and y are cumulative increments of DIC (μmol/kg) from dissolution of carbonate minerals and oxidation of organic matter, respectively, during the transport of the water sample from its surface source region to the sampling position. Equations (4a) to (4c) are the generalized expressions of those originally given by Chen and Pytkowicz (1979). One should be aware of the fact that DIC^0 for the deep waters mostly represents the pre-industrial value. In contrast, DIC^0 for the shallow waters today already contains some additional anthropogenic inputs and may increase with time. Anthropogenic CO_2 does not affect Alk^0 of the surface waters, therefore, Alk^0 is a conservative tracer and probably does not change much with time.

By eliminating x and y from Equations (4a) to (4c), one obtains:

$$(\mathrm{DIC} - \mathrm{Alk}/2) = (\mathrm{DIC}^0 - \mathrm{Alk}^0/2) + [(0.5a + 1)/r_c] \cdot \mathrm{AOU}. \tag{5a}$$

For abbreviation, let DIC − Alk/2 = “DA” (taking the first character of DIC and Alk), so DA^0 (=$\mathrm{DIC}^0 - \mathrm{Alk}^0/2$) is the preformed DA. Variation of DA is now only tied to oxidation of organic carbon and mixing of water masses. Like any other preformed parameter, DA^0 is also a conservative tracer that changes in the water column only through water mass mixing in the pre-industrial time. However, DA^0 is no longer a conservative tracer for the shallow waters where DIC^0 changes with time due to anthropogenic CO_2 inputs. DA^0 for any deep water sample on the linear segment of the mixing curve again can be expressed by:

$$\mathrm{DA}^0 = f \cdot \mathrm{DA}_1^0 + (1 - f) \cdot \mathrm{DA}_2^0. \tag{5b}$$

By substituting Equations (1) and (5b) into Equation (5a), one obtains:

$$\mathrm{DA} = \beta_0 + \beta_1 \cdot \theta + \beta_2 \cdot \mathrm{AOU}, \tag{5c}$$

where

$$\beta_0 = \mathrm{DA}_2^0 - (\mathrm{DA}_1^0 - \mathrm{DA}_2^0) \cdot \theta_2/(\theta_1 - \theta_2),$$

$$\beta_1 = (\mathrm{DA}_1^0 - \mathrm{DA}_2^0)/(\theta_1 - \theta_2),$$

and

$$\beta_2 = (0.5a + 1)/r_c = [0.5(r_c/r_n + r_c/r_p) + 1]/r_c,$$

thus,

$$r_c = 1/[\beta_2 - 0.5(1/r_n + 1/r_p)]. \tag{5d}$$

By the multiple linear regression of DA (=DIC − Alk/2), θ, and AOU data from the linear segment of the mixing curve for deep waters, one can obtain β_0, β_1, and β_2; thus, r_c.

There is one small complication in our model. For example, one can rewrite Equation (2c) to make NO_3 as a dependent variable, i.e.,

$$\mathrm{NO_3} = \alpha_o/r_n + \alpha_1/r_n \cdot \theta - 1/r_n \cdot \mathrm{O_2}. \tag{5e}$$

By the multiple linear regression of NO_3, θ, and O_2 concentration data, one can get $1/r_n$, thus, its inverse, designated as r_n'. The problem is that r_n' is equal to r_n only if the square of the multiple correlation (R^2) is equal to one. However, by eliminating a few obvious outliers, one can easily obtain R^2 greater than 0.98 to 0.99 for most cases. When R^2 is greater than 0.99, $r_n \pm \Delta r_n$ and $r_n' \pm \Delta r_n'$ values usually overlap each other, where Δr_n and $\Delta r_n'$ are the standard errors of r_n and r_n' respectively. The final results given in Table I are the averaged value, i.e. $(r_n + r_n')/2$ with an estimated uncertainty of $\pm[(\Delta r_n)^2 + (\Delta r_n')^2]^{1/2}/2$. Similarly, r_p' and r_c' were also obtained and the final results are expressed as the averaged values of r_p and r_p', and r_c and r_c'. Our model also can fit equally well to the data set along any isopycnal horizon, neutral surface, and even isobaric or equal water depth horizon in deep oceans as long as the $S - \theta$ plot is linear within errors of the data between the two end members.

Once r_n, r_p and r_c are known, and if Alk^0 is given, then from Equations (4a) to (4c), one obtains:

$$y = \mathrm{AOU}/r_c, \tag{6a}$$

$$x = (\mathrm{Alk} - \mathrm{Alk}^0)/2 + 0.5a \cdot \mathrm{AOU}/r_c, \tag{6b}$$

and

$$\mathrm{DIC}^0 = \mathrm{DIC} - (\mathrm{Alk} - \mathrm{Alk}^0)/2 - (1 + 0.5a) \cdot \mathrm{AOU}/r_c, \tag{6c}$$

where DIC^0 is the DIC corrected for the changes caused by dissolution of carbonate and oxidation of organic matter. Therefore, DIC^0 contains only the pre-industrial DIC and the anthropogenic CO_2 components. For the deep waters, the anthropogenic CO_2 component is often negligible.

For comparison, the two end-member mixing model given by Takahashi et al. (1985) and Broecker et al. (1985) essentially also started from Equations (1) and (2a), except that they expanded Equation (2a) into:

$$O_2 + r_n \cdot NO_3 = f \cdot [(O_2)_1 + r_n \cdot (NO_3)_1] + (1 - f) \cdot [(O_2)_2 + (NO_3)_2]. \quad (7a)$$

By rearranging Equation (7a), one obtains:

$$r_n = [-O_2 + f \cdot (O_2)_1 + (O_2)_2 - f \cdot (O_2)_2]/[NO_3 - f \cdot (NO_3)_1 - (NO_3)_2 + f \cdot (NO_3)_2], \quad (7b)$$

where $f = (\theta - \theta_2)/(\theta_1 - \theta_2)$. Therefore, to obtain r_n value for each sample, one needs to know the end member values for θ, O_2, and NO_3. The procedures for obtaining these end member values (Takahashi et al, 1985) may introduce additional uncertainties (Minster and Boulahadid, 1987). In contrast, our model here does not require this step.

For the two end member mixing, Minster and Boulahadid (1987) introduced the following four equations:

$$\theta = f \cdot \theta_1 + (1 - f) \cdot \theta_2, \quad (8a)$$

$$AOU = f \cdot AOU_1 + (1 - f) \cdot AOU_2 + \Delta AOU, \quad (8b)$$

$$NO_3 = f \cdot (NO_3)_1 + (1 - f) \cdot (NO_3)_2 + \Delta AOU/r_n, \quad (8c)$$

$$PO_4 = f \cdot (PO_4)_1 + (1 - f) \cdot (PO_4)_2 + \Delta AOU/r_p. \quad (8d)$$

Therefore, if the end member values for θ, AOU, NO_3, and PO_4 are known, the f and ΔAOU values for any individual sample and the best values of r_n and r_p for the sample set can be obtained by the nonlinear inverse technique (Tarantola and Valette, 1982). The disadvantage of this approach is again that the chosen end member values easily bias the estimates of f, ΔAOU, r_n and r_p values. In order to avoid this pitfall, Anderson and Sarmiento (1994) introduced an additional two equations analogous to Equations (8c) and (8d) for DIC and Alk, and assumed ΔC_{inorg} (carbon increment from dissolution of carbonates) to be proportional to ΔP (phosphate increment from oxidation of organic material). There are now more than enough equations such that the end member values for θ, O_2, NO_3, PO_4, DIC, and Alk along with r_n, r_p, and r_c can be all treated as unknowns, and can be solved simultaneously by the nonlinear inverse technique. However, their assumption (Anderson and Sarmiento, 1994) is not a realistic one. Furthermore, with so many unknowns, the uncertainties of unknown parameters are hard to estimate statistically and the results become very sensitive to the choice of sample combinations for the model fitting. In contrast, there are only three unknowns in our

two end member model. The least square multiple-linear regression automatically provides the uncertainties of each unknown and easily identifies which data are obvious outliers.

3. Brief Summary of Hydrography and Nutrient Data at Station ALOHA

Station ALOHA is located at 22°45′ N and 158°00′ W, about 100 km north of Oahu, Hawaii. The station has been occupied almost monthly since 1988 to make repeated observations on the physical, chemical, and biological parameters in the water column (Karl and Lukas, 1996). The HOT program data are available via the worldwide internet system using anonymous ftp (Karl and Lukas, 1996). The salinity, potential temperature, and nutrient data from nine HOT cruises conducted in 1994 are all plotted in Figures 1–3 for purposes of illustrating the vertical distribution of water masses and water column properties. We selected only the data which are designated as "good" in the data quality assessment. The range of concentrations and estimated analytical precision (as standard deviation) for the following parameters are: θ = (1 to 26) $\pm$ 0.001 °C; S = (34 to 35.4) $\pm$ 0.001 per mil; O_2 = (20 to 230) $\pm$ 0.2 μmol/kg; PO_4 = (0 to 3.2) $\pm$ 0.01 μmol/kg; NO_3 = (0 to 43) $\pm$ 0.05 μmol/kg; DIC = (1970 to 2400) $\pm$ 1 μmol/kg; and Alk = (2280 to 2460) $\pm$ 5 μeq/kg. The ratios of standard deviation to the difference between the highest and lowest concentrations for the above parameters are respectively 0.004, 0.07, 0.1, 0.31, 0.12, 0.23, and 2.8%. Therefore, alkalinity has the most and θ the least noisy data.

The numerals 1 to 6 in Figures 1a and 1b represent the following water-mass end-members: (1) North Pacific Bottom Water (NPBW) at a depth of about 4800 m, (2) North Pacific Deep Water (NPDW; 1000 $\pm$ 50 m), (3) low salinity North Pacific Intermediate Water (NPIW; 500 $\pm$ 50 m), (4) Shallow Salinity Minimum Water (SSMW; 320 $\pm$ 30 m), (5) Subtropical Salinity Maximum Water (STMW; 150 $\pm$ 30 m), and (6) the Surface Water (Sabine et al., 1995). Segment I in Figure 1a represents water samples between the end-members 1 and 2, segment II, between the end-members 2 and 3, and so forth. Each segment is assigned a different symbol in all figures throughout this paper for ease of identification. Figure 1b is a plot of salinity versus water depth to show the relative volume of different water masses at station ALOHA. Segment I has by far the largest volume, but the smallest ranges in θ and S. The origin and temporal variability of water properties of the Subtropical Salinity Maximum Water, Intermediate Waters, and the Deep and Bottom Waters at station ALOHA are discussed by Bingham and Lukas (1996), Kennan and Lukas (1996), Lukas and Santiago-Mandujano (1996), and references therein. The Subtropical Salinity Maximum Water originates near the North Pacific subtropical front at 25 °N to 30 °N, where evaporation exceeds precipitation. The Shallow Salinity Minimum Water is high in oxygen and is formed by the wind-driven circulation in the eastern North Pacific (Talley, 1985). The North Pacific Intermediate Water forms in the mixing region of the Kuroshio and Oyashio currents off the

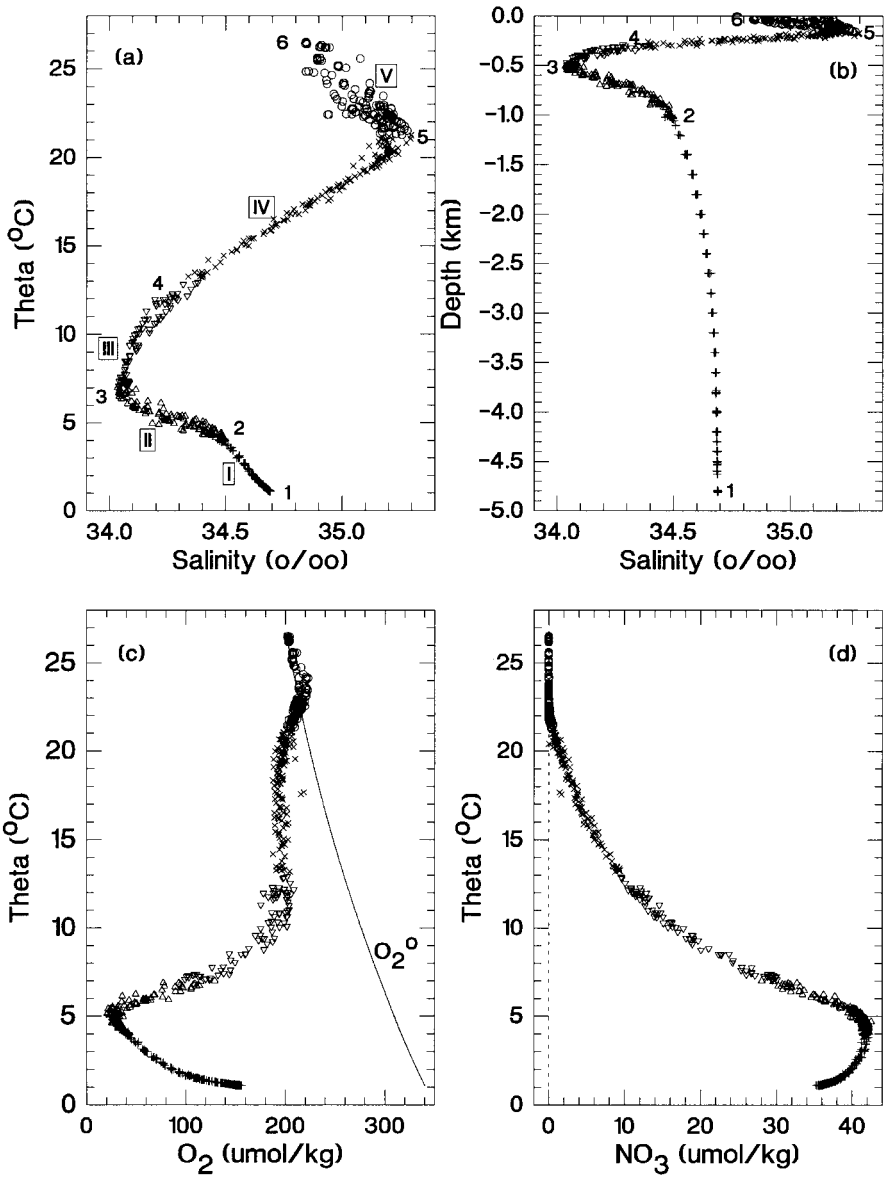

Figure 1. Various *XY* plots among salinity (S), potential temperature (θ), dissolved oxygen (O_2), dissolved NO_3 (analytically includes both nitrate and nitrite), and water depth for the HOT-1994 data. Arabic numerals 1 to 6 in Figures 1a and 1b represent the known end-members of water masses (see the text for the details). The water masses between two end-members are designated by Roman numerals I to V and by different symbols. The solid line in Figure 1c represents the saturated oxygen concentration (O_2^0) at the given θ and S of each water sample.

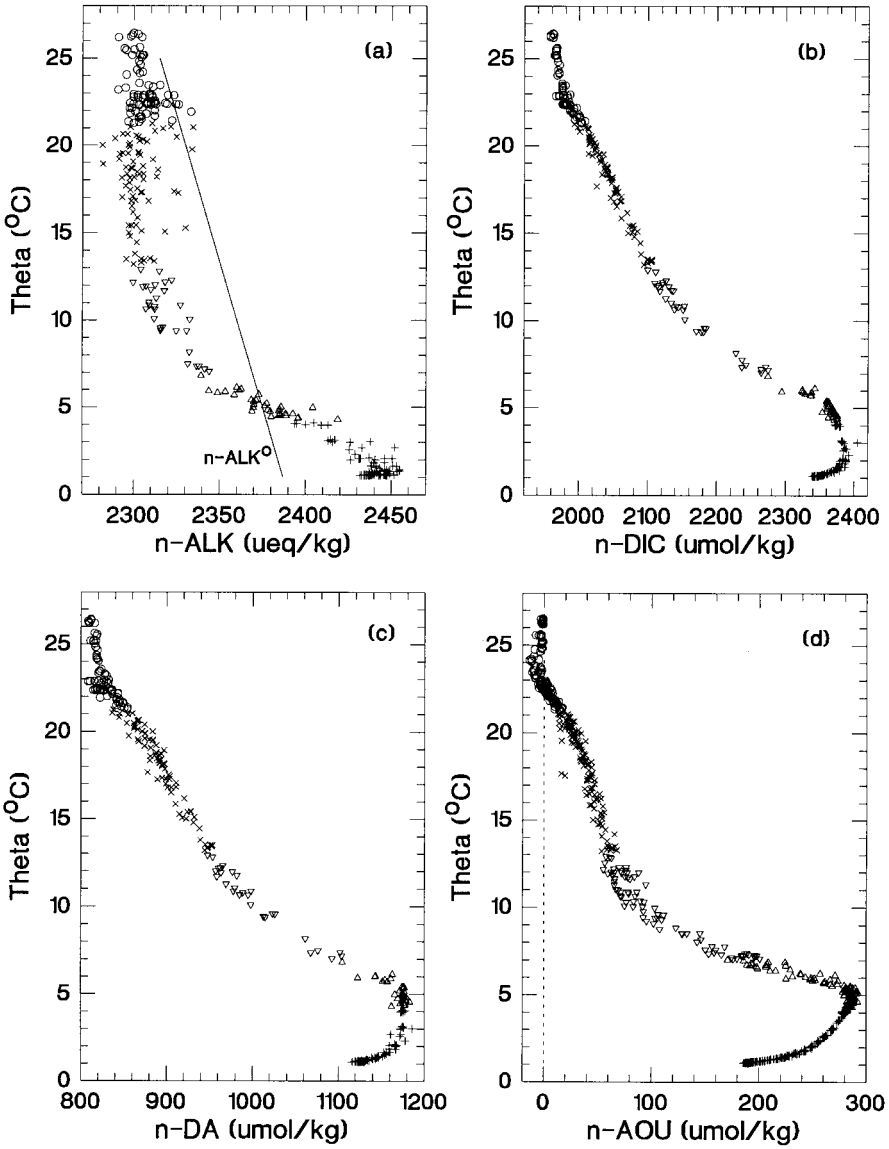

Figure 2. The plots of potential temperature (θ) versus (a) normalized alkalinity (n-Alk), (b), normalized total dissolved inorganic carbon (n-DIC), (c) normalized DA (= n-DIC − n-Alk/2), and (d) normalized apparent oxygen utilization (n-AOU) for the HOT-1994 data. Symbols are the same as in Figure 1. The solid line (n-Alk^0) in Figure 2a represents Equation (9) in the text.

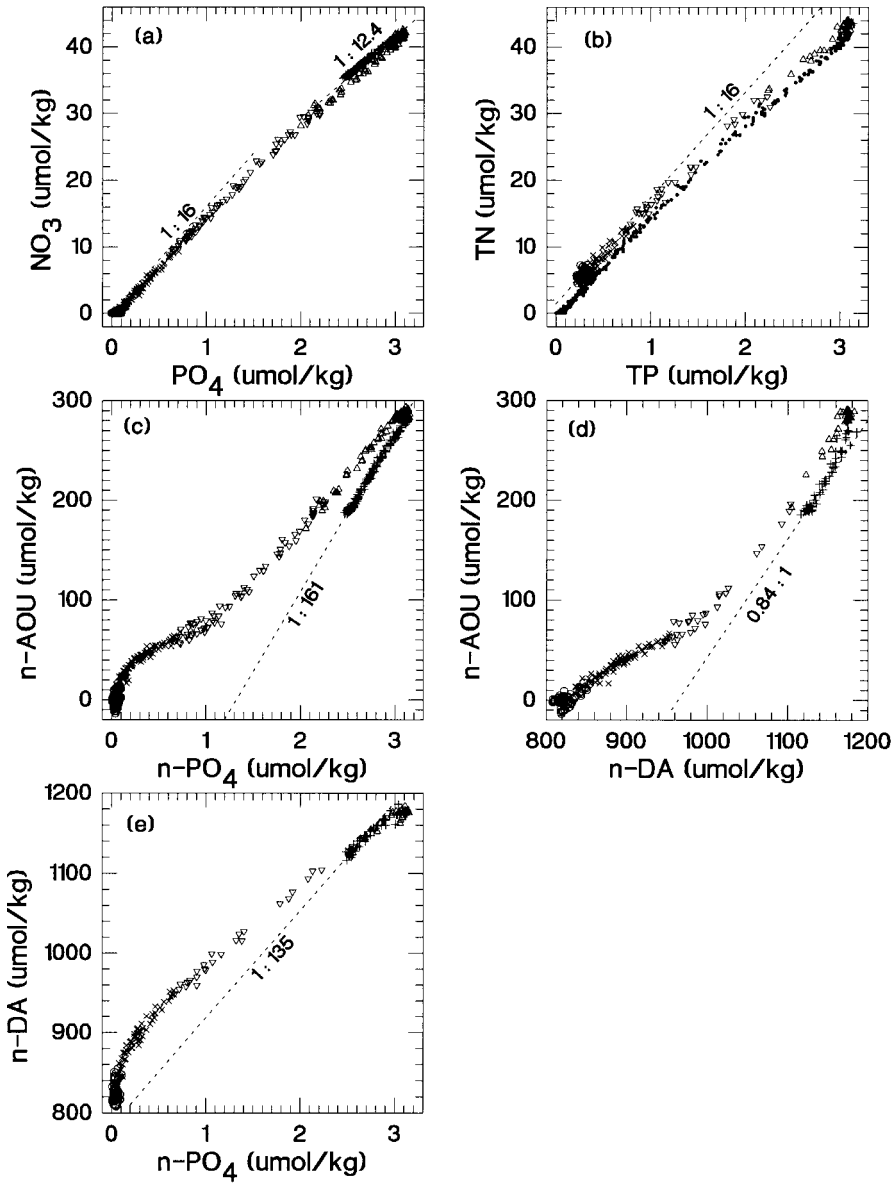

Figure 3. Various XY plots among PO_4, NO_3, TP (=PO_4 + dissolved organic P), TN (=NO_3 + dissolved organic N), n-AOU, n-DA, and n-PO_4 for the HOT-1994 data. The dashed lines passing through segment I data have the following slopes from the model: r_p/r_n = 12.4 in Figure 3a, r_p = 161 in Figure 3c, $1/[(0.5a+1)/r_c]$ = 1/0.84 in Figure 3d, and $r_p/[(0.5a+1)/r_c]$ = 135 in Figure 3e. Symbols are the same as in Figure 1 except small solid circles in Figure 3b, which is a reproduction of Figure 3a (excluding segment I data).

Kuril Islands and Japan (Talley et al., 1995). Segments I and IV are fairly linear in the θ-S plot (Figure 1a); thus, these are suitable for modeling purposes. Segments II, III, and V show greater variability and probable mixing of more than two water-mass end-members.

The well-defined O_2 minimum centers around θ = 5 °C or at a depth of 750 $\pm$ 50 m (Figure 1c). The difference between the saturated O_2 (the solid line in Figure 1c) and the observed O_2 concentration corresponds to the apparent oxygen utilization (AOU). The surface waters are saturated with respect to O_2, but the subsurface waters in segment V tend to be slightly supersaturated; thus, they have negative AOU values. Nitrate concentrations are consistently low in the surface layer (segment V in Figure 1d), and increase with depth to the oxygen minimum, then decrease toward the bottom. The phosphate profile is similar to that of nitrate; thus, it is not shown here.

It is customary to normalize the Alk and DIC data to salinity 35 by multiplying by the factor 35/S, even though this normalizing step is unnecessary for our two end member mixing model. The purpose is to present the data more coherently in a graphic form by excluding any change caused by removal or input of water through evaporation or precipitation. For consistency, other parameters are also normalized to salinity 35 whenever they are compared with the normalized Alk and DIC (n-Alk and n-DIC), even though the corrections are minor. Hereafter, the prefix "n-" always represents the salinity-normalized quantity. Normalized alkalinities (n-Alk) have a low value of about 2300 μeq/kg from the surface to a water depth of about 400 m ($\theta \approx$10 °C), then increase nearly linearly toward to the bottom (Figure 2a). The n-DIC, n-DA, and n-AOU are nearly constant from the surface to a water depth of 100 m (θ between 23 and 26 °C), then increase with depth to about 1000 m, below which all these normalized quantities decrease toward the bottom with different decreasing patterns (Figures 2b to 2d). The n-Alk data tend to be more variable than the others, as mentioned earlier. The solid line in Figure 2a is the normalized preformed alkalinity (n-Alk^0) for the surface Pacific Ocean (Chen, 1982), and will be discussed later.

The plot of PO_4 versus NO_3 (Figure 3a; analytically NO_3 includes both nitrate and nitrite) shows a decreasing trend of the N/P slope from the surface value of 16 to the bottom value of about 12.4. This trend holds also in the plot of total phosphorus (PO_4 + dissolved organic P) versus total nitrogen (NO_3 + dissolved organic N) in Figure 3b, but with a larger non-zero intercept as also shown by Karl et al. (1993). The small solid circles in Figure 3b are essentially the replicate of Figure 3a, except that the data from segment I are omitted because there is no dissolved organic P and N data for segment I. Figures 3c to 3e show the different correlation patterns among n-DA, n-AOU, and n-PO_4 (or n-NO_3) in the water column. The dashed lines passing through the segment I data with different slopes in Figures 3a and 3c to 3e will be discussed later.

4. Results and Discussion

By fitting the O_2, θ, and NO_3 concentration data from segment I into Equations (2c) and (5e), one obtains an averaged r_n = 13.0 ± 0.4. Adapting this value, the "NO" (=O_2 + $r_n \cdot NO_3$) values for all samples were calculated and plotted in Figure 4a. One interesting outcome is that segments II + III also form a straight line in the plot of "NO" versus θ (Figure 4a). The implication is that segments II + III also may have formed by two end-member mixing with regard to "NO" and θ, and should have an averaged r_n value similar to 13.0 ± 0.4. Segment IV data define a straight line in the S-θ plot (Figure 1a); therefore, the O_2, θ, and NO_3 data can also be fitted to our model. Furthermore, since the range of variation of the O_2 concentrations is small in this segment (Figure 1c), the fitting of data to Equation (2c) is never satisfactory ($R^2 \approx 0.7$), but Equation (5e) improves the fitting drastically ($R^2 \approx$ 0.99). The obtained r_n' is 12.3 ± 1.0, which is in agreement with the averaged value of 13.0 ± 0.4 for segment I within the estimated uncertainty. Therefore, as a first approximation, one can consider the averaged r_n nearly constant with depth, as also shown by Broecker et al. (1985) for the three major ocean basins. Additional calculations using the data from HOT-1993 cruises confirm this conclusion (Table Ia). Our value here, however, is much higher than the traditional Redfield ratio of 8.6 (Table Ia).

The difference between the O_2 saturation line (O_2^0) and the calculated "NO" values (symbols) in Figure 4a divided by r_n corresponds to the preformed nitrate (NO_3^0). These values are plotted in Figure 4b. Interestingly, NO_3^0 in segment I is nearly constant with depth. As shown in Figure 1d, the NO_3 concentrations in the surface layer (i.e., segment V) are already vanishingly small, even though the dissolved organic nitrogen (DON) can be as high as 6 to 8 μmol/kg. Therefore, any appreciable positive or negative NO_3^0 values in segment V are mainly caused by the supersaturation or undersaturation of oxygen, and these data are not shown in Figure 4b. The negative NO_3^0 values between θ = 19 and 21 °C in segment IV (Figure 4b) may indicate some undersaturation of oxygen in the surface source region(s) of those waters. Emerson and Hayward (1995) also detected this negative NO_3^0 in North Pacific waters.

Similar calculations for the PO_4 data give an averaged r_p value equal to 161 ± 8 for segment I, and r_p' value of 171 ± 21 for segment IV data from HOT-1994 cruises. Again, the averaged r_p values are nearly constant with depth (Table Ia). The "PO" and PO_4^0 values calculated from adopting r_p =161 are plotted against "NO" and NO_3^0 in Figures 4c and 4d, respectively. The tight linear relationships between "PO" and "NO", and between PO_4^0 and NO_3^0 (including the negative values for both PO_4^0 and NO_3^0) as shown in Figures 4c and 4d confirm the nearly identical geochemical behavior of nitrate and phosphate in the Pacific Ocean below the surface layer. There is no direct evidence to suggest any fractionation between "PO" and "NO" or between PO_4^0 and NO_3^0 due to denitrification processes and/or by the respiration of nitrogen-poor organic matter from the surface oceans as proposed

Table I. (A) Comparison between Redfield ratios and the water column remineralization ratios at station ALOHA in the north Pacific Ocean at different potential temperature (θ) and depth intervals, and (B) the remineralization ratios along the isopycnal horizons of σ_4 = 45.86 in the deep Pacific Ocean, of σ_4 = 45.94 in the deep Indian Ocean, and σ_θ = 27.20 in the Atlantic and Indian Oceans

Data set(s)	θ (°C)	Depth (m)	$r_p = -O_2/P$	$r_n = -O_2/N$	β_2	$r_c = -O_2/C_{org}$	$a = H^+/C_{org}$	$P/N/C_{org}/-O_2$
(A)								
Redfield			138	8.63	0.83	1.30	0.160	1/16/106/138
Hot '94 seg. I	1.1–4.1	4800–1000	161 ± 8	13.0 ± 0.4	0.84 ± 0.04	1.25 ± 0.07	0.104 ± 0.009	1/12.4 ± 0.7/129 ± 11/161 ± 8
Hot '94 seg. IV	13.3–19.1	300–210	(171 ± 21)	(12.3 ± 1.0)				1/13.9 ± 2.1/?/171 ± 2
Hot '93 seg. I	1.1–4.2	4800–900	178 ± 9	13.0 ± 0.3	0.84 ± 0.07	1.25 ± 0.12	0.103 ± 0.013	1/13.7 ± 0.8/142 ± 15/178 ± 9
Hot '93 seg. IV	13.0–19.5	280–140	(186 ± 29)	(13.2 ± 2.0)				1/14.1 ± 3.1/?/186 ± 29
(B)								
deep	1.36–1.51	≈3000	168 ± 10	13.0 ± 0.9	0.66 ± 0.10	1.62 ± 0.29	0.134 ± 0.026	1/12.9 ± 1.1/104 ± 20/168 ± 10
Pacific								[1/14.8 ± 1.0/130 ± 16/199 ± 10]
deep	1.20–1.26	≈3300	171 ± 17	12.8 ± 0.9	0.89 ± 0.15	1.18 ± 0.30	0.099 ± 0.026	1/13.4 ± 1.6/145 ± 40/171 ± 17
Indian								[1/13.4 ± 1.0/135 ± 18/176 ± 11]
Indian	6.5–16.9	730–250	178 ± 7	11.0 ± 0.4	0.66 ± 0.04	1.63 ± 0.11	0.157 ± 0.011	1/16.2 ± 0.9/109 ± 9/178 ± 7
								[1/14.5 ± 0.5/125 ± 7/174 ± 6]
Atlantic	2.1–12.4	1000–450	171 ± 2	10.1 ± 0.2	0.60 ± 0.05	1.84 ± 0.14	0.193 ± 0.015	1/16.9 ± 0.4/ 93 ± 8/171 ± 2
								[1/16.8 ± 1.3/ 92 ± 12/178 ± 11]

(A) values in parentheses are r'_p and r'_n.
(B) values in brackets are results given by Peng and Broecker (1987) for the deep Pacific and deep Indian Oceans and by Takahashi et al. (1985) for thermoclines in the Indian and Atlantic Oceans.

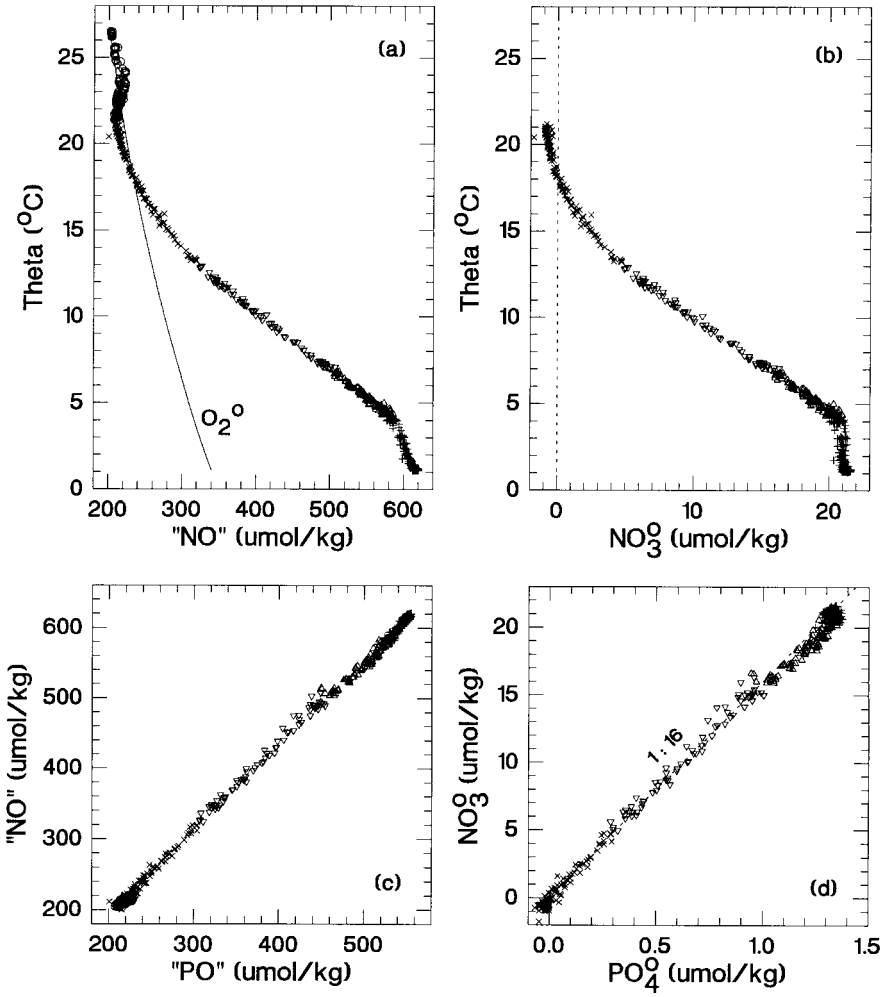

Figure 4. Various XY plots among θ, "NO" (=$O_2 + r_n \cdot NO_3$), NO_3^0 (=$NO_3 - AOU/r_n$), "PO" (=$O_2 + r_p \cdot PO_4$), and PO_4^0 (=$PO_4 - AOU/r_p$) for the HOT-1994 data. The solid line in Figure 4a is the saturated O_2 (O_2^0) at the given θ and S of water samples. Symbols are the same as in Figure 1.

by Emerson and Hayward (1995). The PO_4^0 values are also nearly constant within segment I. However, the N/P ratio of remineralization (= r_p/r_n) for segment I is 12.4 ± 0.7, which is different from the slope of 16 in the plot of NO_3^0 versus PO_4^0 (Figure 4d, where the intercept is zero, thus, the slope and the ratio are the same) and the traditional Redfield N/P ratio. The higher N/P ratio of NO_3^0/PO_4^0 than that of remineralization may suggest the following: Plankton may have a N/P ratio of about 16 originally and P is preferentially remineralized over N. If this is true, one expects the observed lower N/P ratio of remineralization and a higher N/P ratio for

the residual organic matter. As shown by Christian et al. (1997), the sediment trap material collected at the depth interval between 150 and 500 m at station ALOHA indeed have high N/P ratios of 19 to 23.5. One may expect, however, that a significant fraction of organic N in the settling materials is converted to dinitrogen during the nitrification and denitrification processes in the water column and/or more likely in the bottom sediments in order to maintain the observed low N/P ratio of remineralization in the water column. If this is true for the whole ocean, the surface ocean should also gain extra fixed nitrogen through biological nitrogen fixation processes (Karl et al.,1996) in order to maintain a steady state budget of fixed nitrogen in the ocean. Further studies are certainly needed. The C_{org}/N ratio of remineralization (= r_n/r_c = 9 to 10, Table Ia) and the C_{org}/N ratio in the sediment trap material (= 8 to 12; Karl et al., 1995, and Christian et al., 1997) are similar. Therefore, the fractionation between N and C_{org} is probably relatively small during the remineraliztion of plankton in the water column at station ALOHA.

The averaged β_2 (=$[1 + a/2]/r_c$) and r_c values obtained by the multiple linear regression of DA, θ, and AOU data from segment I according to Equation (5c) and the corresponding equation with AOU as the dependent variable are given in Table Ia. Those values are again probably independent of depth, though there are no real data to prove the notion. Because the averaged r_p, r_n, and r_c are all known, the remineralization ratios of P/N/C_{org}/–O_2 can be estimated and are summarized in Table Ia. The remineralization ratios obtained from the HOT data agree with one another within estimated uncertainties. The average for segment I gives P/N/C_{org}/–O_2 = 1/13 ± 1/135 ± 18/170 ± 9, which is different from the traditional Redfield ratios (1/16/106/138). However, without knowing uncertainties of the traditional Redfield ratios, it is hard to place any significance on the differences. The P/N/C_{org} ratios for the suspended organic particulate matter (mostly living plankton) in the surface waters at station ALOHA are equal to 1/14.2 ± 3.3/112 ± 32 (Karl et al., 1995), which are again in agreement with the remineralization ratios obtained for segment I within estimated uncertainties. Based on about one hundred chemical composition data of phytoplankton from the literature, Duarte (1992) gave the average concentrations of C_{org} = 28 ± 10, N = 3.9 ± 1.8 and P = 0.37 ± 0.45 mmol/g dry phytoplankton. The high standard deviation for phosphorus data is caused by 10 samples with extremely high P contents (0.68 to 2.7 mmol/g dry phytoplankton). If one excludes those samples, the average P content reduces to 0.25 ± 0.13 mmol/g with much smaller standard deviation. Using this new estimate of P content, the P/N/C_{org} ratios become 1/15 ± 10/110 ± 69, which are very similar to the traditional Redfield ratios (1/16/106), but have much larger standard deviations than those for the remineralization ratios given here. The large standard deviations reflect the facts that logarithms of the C_{org}/N and N/P ratios of phytoplankton (and other aquatic plants) are inversely related to logarithms of N and P contents, respectively (Duarte, 1992), and those ratios are also exponential functions of specific growth rate of phytoplankton (Goldman et al., 1979). Appar-

ently, the remineralization processes in the water column have smoothed out the large variability of plankton compositions.

Based on the remineralization ratios from segment I of the HOT data ($P/N/C_{org}/-O_2 = 1/13/135/170$) and the H/C_{org} ratio of 1.65 for marine phytoplankton (Anderson, 1995), the molar formula of the remineralized plankton may be written as $C_{135}H_{280}O_{105}N_{13}P$ or $C_{25}(CH_2O)_{101}(CH_4)_9(NH_3)_{13}(H_3PO_4)$. Oxidation of this formula results in:

$$C_{135}H_{280}O_{105}N_{13}P + 170O_2 \rightarrow 135CO_2 + 132H_2O + 13NO_3^- + H_2PO_4^- + 14H^+.$$

For comparison, Anderson (1995) gave a formula of $C_{106}H_{175}O_{42}N_{16}P$ or $C_{56}(CH_2O)_{38}(CH_4)_{12}(NH_3)_{16}(H_3PO_4)$. For reference, the "$a$" values ($=H^+/C_{org} = r_c/r_p + r_c/r_n$) are also summarized in Table Ia. The average "a" for segment I of the HOT data is 0.10 ± 0.01, which is much lower than the value of 0.16 for the traditional Redfield ratios. This difference reflects the low nitrogen and high carbon contents in the newly proposed molar formula of remineralized plankton here, as compared to the traditional stoichiometric representation of plankton.

The θ and nutrients data along the isopycnal horizons of $\sigma_\theta = 27.20$ in the Atlantic and Indian thermoclines as given by Takahashi et al.(1985) , and of $\sigma_4 = 45.86$ in the deep Pacific and of $\sigma_4 = 45.94$ in the deep Indian Oceans given by Peng and Broecker (1987), are also fitted to our model. The obtained remineralization ratios are in good agreement with those given by Takahashi et al.(1985) and Peng and Broecker (1987) except for the deep Pacific values, as summarized in Table Ib. However, the β_2, r_c and "a" values obtained for the Indian and Atlantic thermoclines (Table Ib) are in doubt, because our model (Equations (5c) and (5d)) should apply only to the pre-industrial deep waters. As mentioned earlier, the advantage of our model is that it does not require an estimate of the preformed nutrients for the end members first (Takahashi et al., 1985), the so-called f-factor (a measure of the excess oxygen needed to oxidize the hydrogens associated with carbon-bearing compounds) based on the N/P and C/N ratios of sediment trap material (Peng and Broecker, 1987), or to assign the θ, AOU and nutrient concentration values for the end members (Minster and Boulahdid, 1987). The procedures for estimating the preformed nutrients and the f-factor introduce additional uncertainties in the calculations of remineralization ratios (Minster and Boulahdid, 1987). As summarized by Broecker et al. (1985) and supported by the present results (Table Ia and Ib), the r_p seems to be fairly constant (170 ± 10) throughout the three major oceans regardless of water depth. However, we can not conclude the same for the r_n and r_c at the present time. Varying degree of dinitrogen production during denitrification processes may result in higher r_n or lower N/P ratio of remineralization($= r_p/r_n$). Also, possible production of dinitrogen during nitrification processes has never been quantified in the natural environment. Another problem is the systematic errors within the GEOSECS data sets (Broecker et al., 1985) and among different

historic data sets. For example, there are systematic offsets of about 10 μeq/kg in n-Alk and 26 μmol/kg in n-DIC between the GEOSECS Pacific station 212 (closest to station ALOHA) and the HOT-1994 data sets in the depth interval between 1000 and 5000 m. Further study using our two end-member model, its expanded three end-member model, and the WOCE (World Ocean Circulation Experiment) data set is underway.

In segment I, both PO_4^0 and NO_3^0 are nearly constant (Figures 4b and 4d) and the variation range of n-DA^0 is small (not shown here). Therefore, the changes in PO_4, NO_3, and n-DA concentrations in segment I mainly reflect the oxidation of organic matter *in situ* (Sabine et al., 1995). This is confirmed by the overlap of the segment I data and the line with the expected slope obtained from our model as shown in Figures 3a and 3c to 3e. Therefore, in order to obtain a rough estimate of remineralization ratios in the water column, one need only measure the slopes in the plots of n-PO_4 versus n-NO_3, n-DA, and n-AOU data from segment I.

Based on GEOSECS Pacific Expedition (1973–1974) data, Chen (1982) showed that n-Alk^0 in the surface Pacific Ocean is a linear function of θ, i.e.,

$$n\text{-Alk}^0\ (\mu\text{eq/kg}) = (2390\text{–}3.0 \cdot \theta) \pm 10 \tag{9}$$

As mentioned earlier, if the n-Alk^0 is known, the n-x, n-y, and the water column n-DIC^0 can be calculated from Equations (6a) to (6c). As shown in Figure 5a, the n-x values (cumulative increment of n-DIC from dissolution of carbonates) based on the HOT-1994 data set are all negative from the surface down to about 600 $\pm$ 100 m ($\theta \approx 6$ °C in Figure 5a), indicating the net removal of CO_2 by carbonate precipitation in the water column, and increase with depth toward the bottom due to the dissolution of carbonates in the water column as well as at the water–sediment interface. The cross-over of the n-x value at 600 $\pm$ 100 m is consistent with the observation that the degree of saturation with respect to aragonite becomes much less than one at a depth of about 500 m and below at station ALOHA (Sabine et al., 1995; Troy et al., 1997). Also, dissolution of calcite crystals hanging in the water column at station ALOHA starts at 550 $\pm$ 50 m (Troy et al., 1997), even though the degree of saturation with respect to calcite is around one or only slightly less than one at depths between 550 m and 2000 m (Sabine et al., 1995; Troy et al., 1997). The n-y values (cumulative increment of n-DIC from oxidation of organic matter) as calculated from Equation (6a) are nearly zero in surface waters to a depth of 100 m ($\theta \approx 23$ to 26.5 °C in Figure 5a), mainly reflecting the nearly zero value of AOU caused by rapid oxygen gas exchange between the surface ocean and the atmosphere. The n-y value reaches a maximum at the oxygen minimum ($\theta \approx 5$ °C in Figure 5a) and decreases toward the bottom. The previously untested assumption of the proportionality between x and y used by Anderson and Sarmiento (1994) does not hold for the waters at station ALOHA.

In principle, one can estimate the integrated amount of anthropogenic CO_2 in the upper part of water column from the difference between the present water

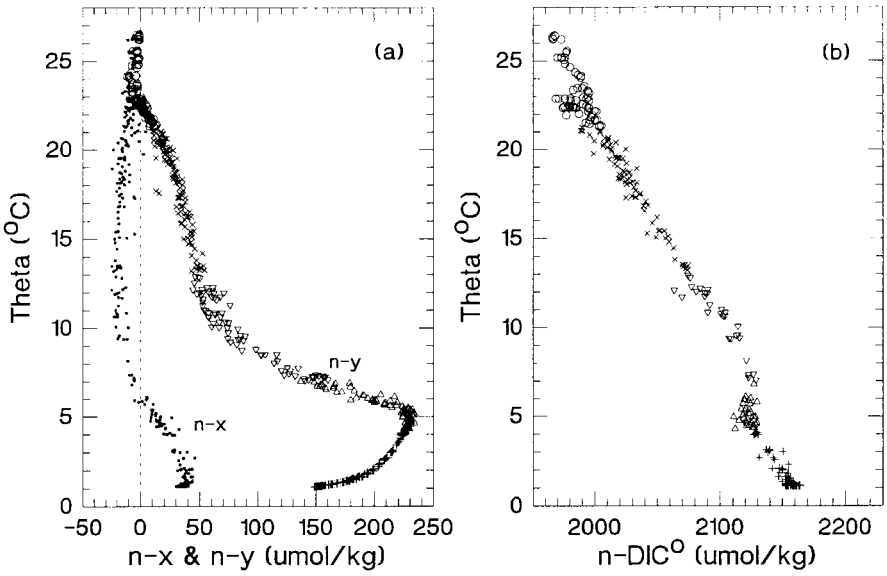

Figure 5. The plots of θ versus (a) n-x and n-y calculated from Equations (6a) and (6b), and (b) the water column n-DIC^0 calculated from Equation (6c) for the HOT-1994 data.

column n-DIC^0 (Figure 5b) and the pre-industrial n-DIC^0. How to estimate the pre-industrial n-DIC^{0}was discussed by Gruber et al. (1996) and is beyond the scope of this paper.

5. Summary and Conclusions

1. A simple two end-member mixing model is developed to estimate the remineralization ratios for marine plankton from a vertical profile data set and from the interpolated data set along an isopycnal or isobaric horizon.
2. By the multiple linear regression of O_2, θ, and PO_4; O_2, θ, and NO_3; and DA, θ, and AOU data sets to the model equations; one can estimate averaged r_p (= –O_2/P), r_n (= –O_2/N), and r_c (= –O_2/C_{org}) values, as well as the remineralization ratios of $P/N/C_{org}/-O_2$ = 1: (r_p/r_n): (r_p/r_c): r_p.
3. The remineralization ratios of $P/N/C_{org}/-O_2$ = 1/13 ± 1/135 ± 18/170 ± 9 are obtained from the HOT-1993 and HOT-1994 data sets. These ratios are comparable to the traditional Redfield ratios ($P/N/C_{org}/-O_2$ = 1/16/106/138), but the latter have large uncertainties of more than 50% when they are based on the average compositions of phytoplankton. Apparently, the remineralization processes in the water column have smoothed out the large variability of plankton compositions.

4. The molar formula of remineralized plankton at station ALOHA can be represented by $C_{135}H_{280}O_{105}N_{13}P$ or $C_{25}(CH_2O)_{101}(CH_4)_9(NH_3)_{13}(H_3PO_4)$, instead of the traditional $(CH_2O)_{106}(NH_3)_{16}(H_3PO_4)$. Oxidation of the new formula results in:

   $$C_{135}H_{280}O_{105}N_{13}P + 170O_2 \rightarrow 135CO_2 + 132H_2O + 13NO_3^- + H_2PO_4^- + 14H^+.$$

5. The N/P ratio of remineralization (= r_p/r_n = 13 $\pm$ 1) is lower than the ratio of 16 for NO_3^0/PO_4^0 at station ALOHA (Figure 4d), implying preferential remineralization of P over N in the water column and partial conversion of organic/inorganic nitrogen into dinitrogen (N_2) in the water column and/or more likely in the bottom sediments. For a steady state ocean, the importation of fixed nitrogen through biological nitrogen fixation processes in the surface oceans is also required to balance the denitrification loss.
6. The r_p is fairly constant (= 170 $\pm$ 10) for the three major oceans regardless of water depth. One may not conclude the same for the r_n and r_c. Production of dinitrogen during denitrification processes can locally result in higher r_n or lower N/P ratio of remineralization (= r_p/r_n). The calibration errors among different data sets, especially for DIC and Alk measurements, may also cause the r_c to vary.
7. There is no direct correlation between the extent of carbonate dissolution and that of organic matter oxidation in the water column at station ALOHA.

Acknowledgments

The authors thank the HOT program participants and staff for their help with sample collections and analyses, and especially D. Hebel, L. Tupas and F. Santiago-Mandujano for their leadership roles as chief scientists on these cruises. This research was supported, in part, by NSF grants OCE-93-15312 (awarded to YHL and CDW), INT94-17480 (awarded to YHL), OCE-93-01368 (awarded to DMK) and OCE-93-03094 (awarded to Roger Lukas). SOEST contribution # 4918 and U.S. JGOFS contribution # 544.

References

Anderson, L. A. and Sarmiento, J. L. (1994) Redfield ratios of remineralization determined by nutrient data analysis. *Global Biogeochem. Cycles* **8**, 65–80.

Anderson, L. A. (1995) On the hydrogen and oxygen content of marine phytoplankton. *Deep Sea Res. Part 1* **42**, 1675–1680.

Bingham, F. M. and Lukas, R. (1996) Seasonal cycles of temperature, salinity and dissolved oxygen observed in the Hawaii Ocean Time-series. *Deep Sea Res.* **43**, 199–214.

Boulahdid, M. and Minster, J. F. (1989) Oxygen consumption and nutrient regeneration ratios along isopycnal horizons in the Pacific Ocean. *Mar. Chem.* **26**, 133–153.

Brewer, P. G., Wong, G. T. F., Bacon, M. P., and Spencer, D. W. (1975) An oceanic calcium problem? *Earth Planet. Sci. Lett.* **26**, 81–87.

Broecker, W. S. (1974) 'NO' as a conservative water-mass tracer. *Earth Planet. Sci. Lett.* **23**,100–107.

Broecker, W. S., Takahashi, T., and Takahashi, T. (1985) Sources and flow patterns of deep-ocean waters as deduced from potential temperature, salinity, and initial phosphate concentration. *J. Geophys. Res.* **90**, 6925–6939.

Chen, C. T. A. and Pytkowicz, R. M. (1979) On the total CO_2-titration alkalinity-oxygen system in the Pacific Ocean. *Nature* **281**, 362–365.

Chen, C. T. A. (1982) Oceanic penetration of excess CO_2 in a cross section between Alaska and Hawaii. *Geophys. Res. Lett.* **9**, 117–119.

Christian, J. R., Lewis, M. R., and Karl, D. M. (1997) Vertical fluxes of carbon, nitrogen and phosphorus in the north Pacific subtropical gyre near Hawaii. *J. Geophys. Res.* **102**(C7), 15667–15677.

Duarte, C.M. (1992) Nutrient concentration of aquatic plants: Patterns across species. *Limnol. Oceanogr.* **37**, 882–889.

Emerson, S. and Hayward, T. (1995) Chemical tracers of biological processes in shallow waters of the North Pacific: Preformed nitrate distributions. *J. Mar. Res.* **53**, 499–513.

Fiadeiro, M. and Craig, H. (1978) Three dimensional modeling of tracers in the deep Pacific Ocean, I. Salinity and oxygen. *J. Mar. Res*. **36**, 323–355.

Fleming, R. H. (1940) Composition of plankton and units for reporting populations and production. *Proc. Sixth Pacific Sci. Congr.* **3**, 535–540.

Goldman, J. C., McCarthy, J. J., and Peavey, D. G. (1979) Growth rate influence on the chemical composition of phytoplankton in oceanic waters. *Nature* **279**, 210–215.

Gruber, N., Sarmiento, J. L., and Stocker, T. F. (1996) An improved method for detecting anthropogenic CO_2 in the oceans. *Global Biogeochem. Cycles* **10**, 809–837.

Karl, D. M., Tien, G., Dore, J., and Winn, C. D. (1993) Total dissolved nitrogen and phosphorus concentrations at US JGOFS Station ALOHA: Redfield reconciliation. *Mar. Chem.* **41**, 203–208.

Karl, D. M., Letelier, R., Hebel, D., Tupas, L., Dore, J., Christian, J., and Winn, C. (1995) Ecosystem changes in the North Pacific subtropical gyre attributed to the 1991–92 El Nino. *Nature* **373**, 230–234.

Karl, D. M. and Lukas, R. (1996) The Hawaii Ocean Time-series (HOT) program: Background, rationale and field implementation. *Deep Sea Res.* **43**, 129–156.

Karl, D., Letelier, R., Tupas, L., Dore, J., Christian, J., and Hebel, D. (1997) The role of nitrogen fixation in biogeochemical cycling in the subtropical North Pacific Ocean. *Nature* **388**, 533–538.

Kennan, S. C. and Lukas, R. (1996) Saline intrusions in the intermediate waters north of Oahu, Hawaii. *Deep Sea Res.* **43**, 215–242.

Lukas, R. and Santiago-Mandujano, F. (1996) Interannual variability of Pacific deep- and bottom-waters observed in the Hawaii Ocean Time-series. *Deep Sea Res.* **43**, 243–256.

Minster, J. F. and Boulahdid, M. (1987) Redfield ratios along isopycnal surfaces – A complementary study. *Deep Sea Res.* **34**, 1981–2003.

Peng, T. H. and Broecker, W. S. (1987) C/P ratios in marine detritus. *Global Biogeochem. Cycles* **1**, 155–161.

Redfield, A. C., Ketchum, B. H., and Richards, F. A. (1963) The influence of organisms on the composition of sea-water. In *The Sea, vol. 2* (ed. M. N. Hill), pp. 26–77. Interscience, New York.

Sabine, C. L., Mackenzie, F. T., Winn, C., and Karl, D. M. (1995) Geochemistry of carbon dioxide in seawater at the Hawaii Ocean Time series station, ALOHA. *Global Biogeochem. Cycles* **9**, 637–651.

Takahashi, T., Broecker, W. S., and Langer, S. (1985) Redfield ratio based on chemical data from isopycnal surfaces. *J. Geophys. Res.* **90**, 6907–6924.

Talley, L. D. (1985) Ventilation of the Subtropical North Pacific: The shallow salinity minimum. *J. Phys. Oceanog.* **15**, 633–649.

Talley, L. D., Nagata, Y., Fujimura, M., Iwao, T., Kono, T., Inagake, D., Hirai, M., and Okuda, K. (1995) North Pacific Intermediate Water in the Kuroshio/Oyashio mixed water region. *J. Phys. Oceanog.* **25**, 475–501.

Tarantola, A. and Valette, B. 1982. Generalized nonlinear inverse problems solved using the least squares criterion. *Rev. Geophys. Space Phys.* **20**, 219–232.

Troy, P. J., Li, Y. H., and Mackenzie, F. T. (1997) Changes in surface morphology of calcite exposed to the oceanic water column. *Aquatic Geochemistry* **3**, 1–20.